Oceanologia, 67 (2)/2025, 67205
Polish Academy of Sciences
Institute of Oceanology

https://doi.org/10.5697/DMFV7237

Coupling pattern of estuarine and surf zone longshore currents at tidal frequencies: Case study of S. E. coast of Nigeria

Effiom E. Antia

Abstract
Within the coastal flow-field system, the hydrodynamic coupling between the tidal channel and surf zone is among the most important, implicated in shoreline morphodynamics, river mouth bar dynamics, and the recreational quality of nearshore waters. The nature of the coupling has seldom been empirically evaluated at tidal frequencies spanning lunar cycles. This investigation is directed at filling this gap in information based on 50-day successive tidal cycle flow monitoring in an estuary–surf zone setting, S. E. coast of Nigeria. Results show a reversing flow pattern at all monitoring stations at tidal frequencies. The estuary indicated ebb-asymmetric tidal cycle residual flow velocities which at spring tide (30–38 cm/s range) act as an expanding jet relative to the flanking surf zone residual longshore current counterparts (typically $\leq$ 5 cm/s). The western and eastern flanking surf zones showed westward- and eastward-asymmetric tidal cycle residual flows, respectively with coastwise decreasing asymmetry reflecting the weakening impact of the estuary outflow. Coupling of surf zone – estuarine residual flow vectors indicated a higher frequency of threshold coefficient ($r \geq 0.7$) at ebb than at flood stage. The observed pattern of strong estuarine residual outflow velocities and modally divergent weak surf zone flows is a favourable condition for the estuary mouth bar development. However, the eastward-skewed bar configuration fits more to the effect of eastward-directed momentum flux associated with water mass transport of the obliquely-shoaling southwesterly waves given that breaking wave-generated longshore currents in the western surf zone display a westward-asymmetry over a tidal cycle.

Keywords
Longshore current; Estuarine flow; Surf zone; Tidal cycle; Nigerian coast

Department of Physical Oceanography, Faculty of Oceanography, University of Calabar, PMB 1115 Calabar, Cross River State, Nigeria
Correspondence: e_antia@yahoo.co.uk

Received: 6 June 2024; **revised:** 15 March 2025; **accepted**: 17 March 2025

1. Introduction

Interests in flow interactions in the vicinity of tidal inlets and estuaries derive primarily from the practical importance of navigational safety, defining pathway of dispersion of estuary-emanating effluents in the near- and off-shore waters, and modeling sediment transport processes driving the development, morphodynamics, and configuration of depositional sand bodies associated with the tidal channels. Moreover, the nature of the hydrodynamic coupling impacts on the contiguous shoreline erosion-accretion patterns leading to the development of shoreline offsets as commonly observed on coasts with shore-projecting engineering structures.

While investigations on the configuration and geometry of these sand bodies have provided initial insights into their major processes and possible interactions in a qualitative and semi-quantitative sense (Todd, 1968; Oertel, 1975; Hayes, 1980; Davis and Fox, 1981; FritzGerald, 1984; Sha and van den Berg, 1993; Guillou and Chapalain, 2012), knowledge of the flow field seaward of the tidal channels is mainly theoretical and model-based (Joshi, 1982; Ozsoy and Unluata, 1982; Chao, 1990; Rusu et al., 2011; Dodet et al., 2013; Olabarrieta et al., 2014; Zainescu et al., 2021).

A review report by Anthony (2015) noted a dearth of field-based investigations on the interactive processes at river mouths. It was opined that the interacting processes play crucial roles in the growth and stability of their associated mouth bars, which subsequently become a modulator of the wave and longshore current pattern. In essence, the coupling between a tidal channel and nearshore flows has not been fully espoused in the literature from an empirical time-series perspective. The foundation for unraveling the

pattern of the coupling is monitoring at tidal frequencies in settings characterized by reversing flow directions, which is the focus of this study.

2. Study area and methods

This investigation was conducted on the western (Itak Abasi) and eastern (Ibeno) beaches adjoining the Qua Iboe River estuary, located on the southeastern coast of Nigeria (Figure 1). Monitoring stations W1 and E1 are referred to as western and eastern estuary-proximal stations while W2 and E2 are estuary-distal counterparts. The estuary monitoring station (Q) is within 100 m of the estuary mouth. The coastal setting has a coastal plain physiography, and is typically composed of fine-grained sands. This coastal segment has a moderate wave energy climate (1–1.5 m and 8–12 s modal wave height and period) with prevailing waves being southwesterly.

Tides are semi-diurnal, mesotidal and show a well-marked fortnightly lunar cycle pattern (Figure 2) based on field monitoring at station Q. Flow monitoring was based on the Lagrangian drogue-type technique as described by Hughes (2002). The drogue object in this study was a 7–8 cm diameter Nypa palm fruit placed about 10–20 m from the estuarine shoreline; travel time and direction were tracked over a 10 m distance. In the surf zones, the Nypa palm fruits were placed at a seaward distance of about 10 m from the shoreline and the time duration and direction of drift over a 10 m marked distance on the beach were noted. An average of three observations was usually recorded for all measurements which were simultaneously conducted at all the five established stations (Figure 1) for 50 successive day-light complete tidal cycles at half-hourly intervals between January 30 and March 20, 2012.

3. Results

3.1 Estuarine flow pattern

The tidal cycle variation in flow velocities in the Qua Iboe River estuary is exemplified for successive neap and spring tides in Figure 3a–b. The southward-directed ebb flows during spring tide attained peak velocities of 100–150 cm/s range, while the northward flood flow velocities were typically < 100 cm/s. At neap tide, ebb and flood flow velocities were mostly < 50–75 cm/s. The tidal cycle directional net averaged (residual) flow velocity pattern in the estuary over the study period given in Figure 4 was predominantly southward or ebb-asymmetric. A tendency towards flood-asymmetry was observed during neap tide (February 2, February 16, March 2 and March 16). Maximum residual velocities coincided with spring tides (February 9, February 22 and March 9).

3.2 Surf zone flow pattern

The tidal cycle variation in longshore flow in the western and eastern surf zones at the neap tide and succeeding spring tide is presented in Figure 5a-b for the same southwesterly wave regime. The flow was reversing at both tidal phases, with the western surf zones (estuary-proximal and distal) indicating eastward flow direction during the flooding stage and westward during the ebbing stage. The eastern surf zone showed an inverse direction pattern of the western surf zone during the tidal stages, i.e. westward flow direction at the flooding stage and eastward flow direction at the ebbing stage. The longshore flow velocities in the eastern surf zones were typically < 20 cm/s at both tidal stages while the western surf zone longshore flow velocities were in the 20–40 cm/s range. While the spring tide results in Figure 6a followed the inverse longshore flow direction pattern given in Figure 5, the neap tide results (Figure 6b) showed the flow directions in both the western and eastern surf zones to be synchronous.

The tidal cycle residual flow patterns for the western and eastern surf zones in Figure 7a–d show the residual flow direction to be reversing, with velocities predominantly < 5 cm/s. It is observed that at the western proximal and distal surf zones (Figure 7a–b), the residual longshore flow is westward-asymmetric but with an eastward asymmetry tendency around neap tides. The eastern surf zone showed a pronounced eastward-asymmetric residual flow velocity at the estuary-proximal surf zone (Figure 7c), and a strongly bimodal pattern at the distal surf zone (Figure 7d).

3.3 Estuarine – surf zone flow directional coupling

The scatter plots of the estuarine and surf zone residual longshore flow vectors for 50 tidal cycles are shown in Figure 8a–d. For the western estuary-proximal and distal surf zones (Figure 8a–b), the coupling of the westward surf zone and southward residual flow vectors (W–S) is most pronounced. The eastern estuary-proximal surf zone (Figure 8c) shows the dominance of eastward surf zone and southward residual flow vectors (E–S) coupling, while the distal counterpart shows a bimodal occurrence of W–S and E–S residual flow coupling.

A comparison of residual flow directional coupling for the estuary-proximal western and eastern surf zones given in Figure 9a suggests surf zone flow divergence to be associated with southward-directed residual estuarine outflow. On the eastern surf zone of Ibeno Beach, eastward surf zone residual flow coupling with residual southward estuarine outflow constitutes 74% of the data set, while the western surf zone counterpart of Itak Abasi Beach has 70% westward surf zone flow coupling with the southward residual estuarine outflow. The occurrence of the W–S coupling is relatively consistent in the estuary-distal western surf zone (68%), whereas the eastern counterpart shows a marked decrease in the E–S coupling to 52%. Quite unlike the estuarine outflow, the estuarine inflow (northward directed) showed a $< 10\%$ coupled relationship with the surf zone flow directions.

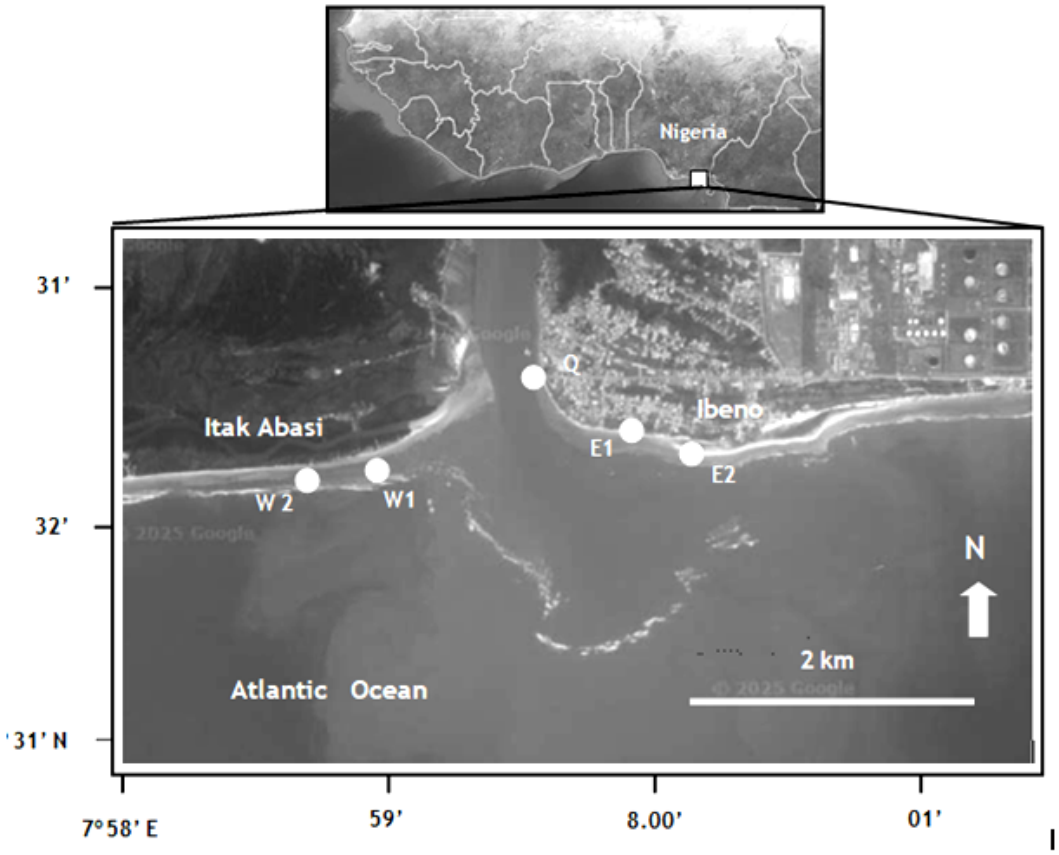

Figure 1. Study location showing Qua Iboe River estuary and the western (Itak Abasi) and eastern (Ibeno) shoreline monitoring stations (Q, W1, W2, E1 and E2) (Google Earth 2013).

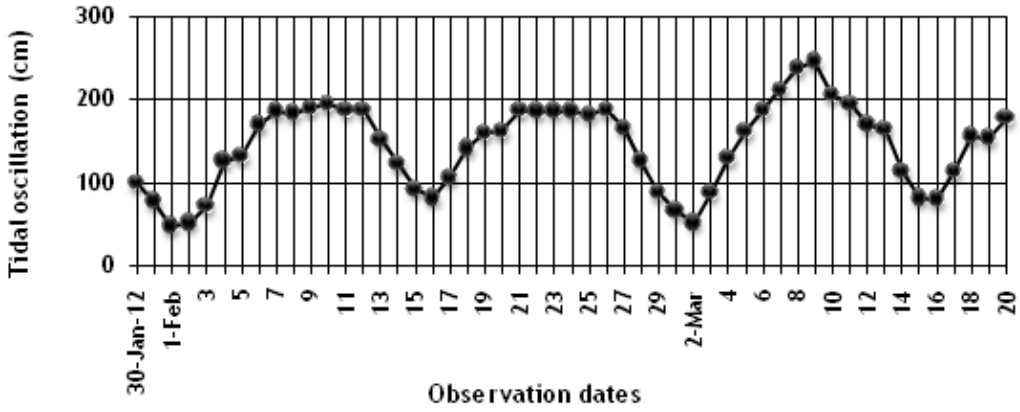

Figure 2. Variation in tidal amplitude of Qua Iboe River estuary during the study period.

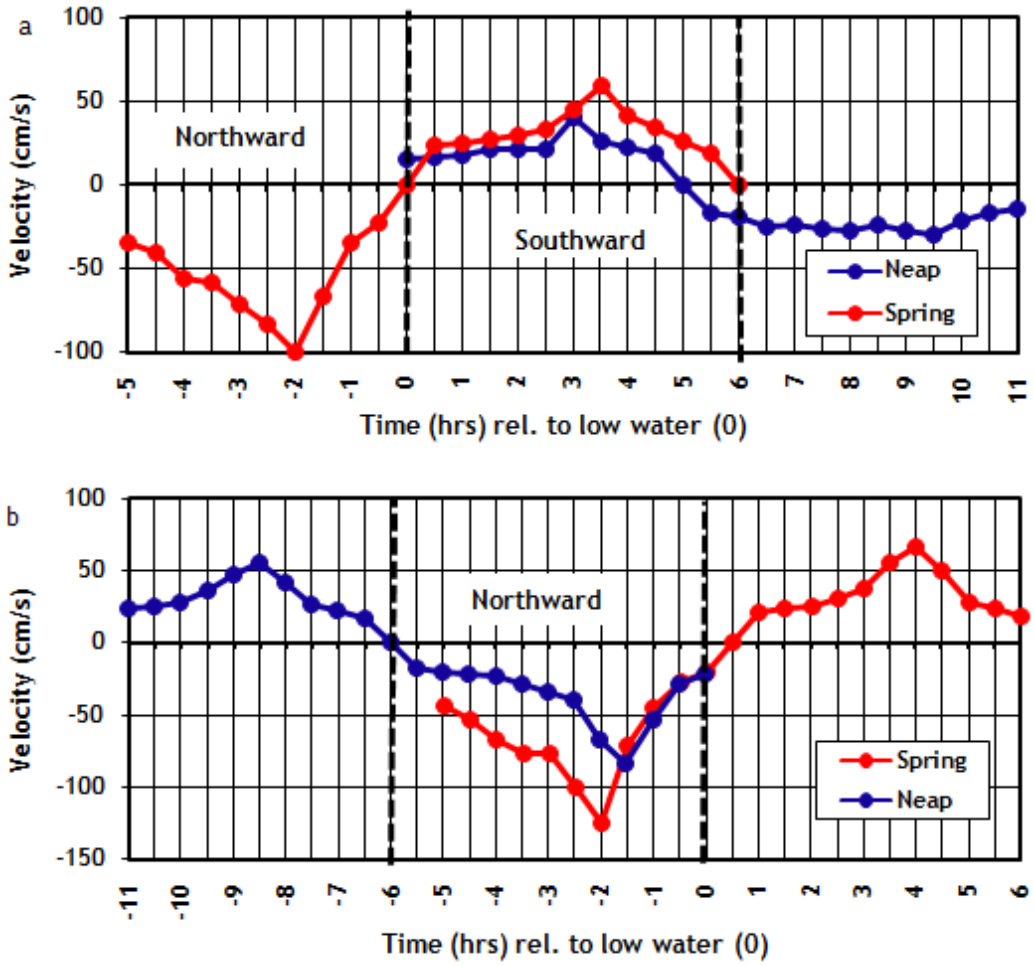

Figure 3. Tidal cycle variation in flow velocities of Qua Iboe River estuary at spring and neap tides of a) February 2 and 8, 2012, b) March 16 and 9, 2012. Vertical discontinuous lines mark low water (0 hr) and high water (± 6 hr).

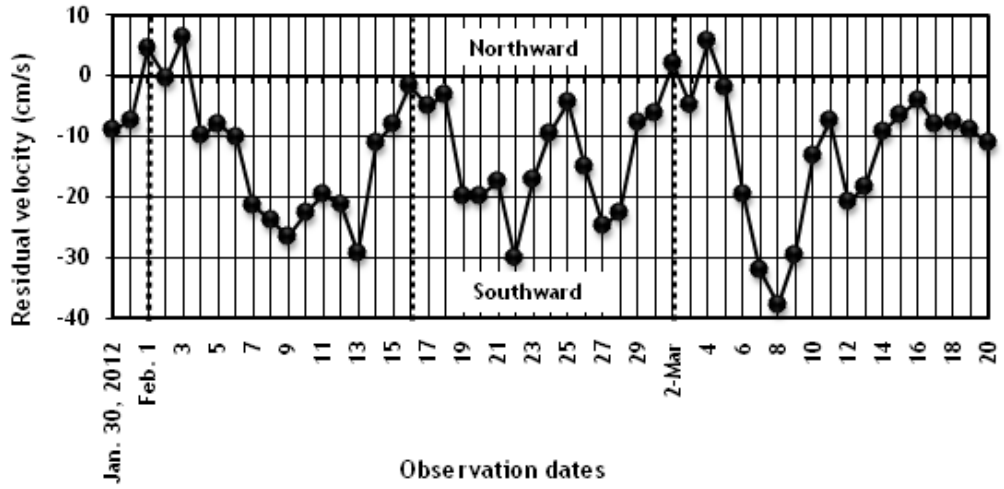

Figure 4. Variation in tidal cycle-averaged net flow velocities of Qua Iboe River estuary (January 30–March 20, 2012). Vertical discontinuous lines mark neap tides.

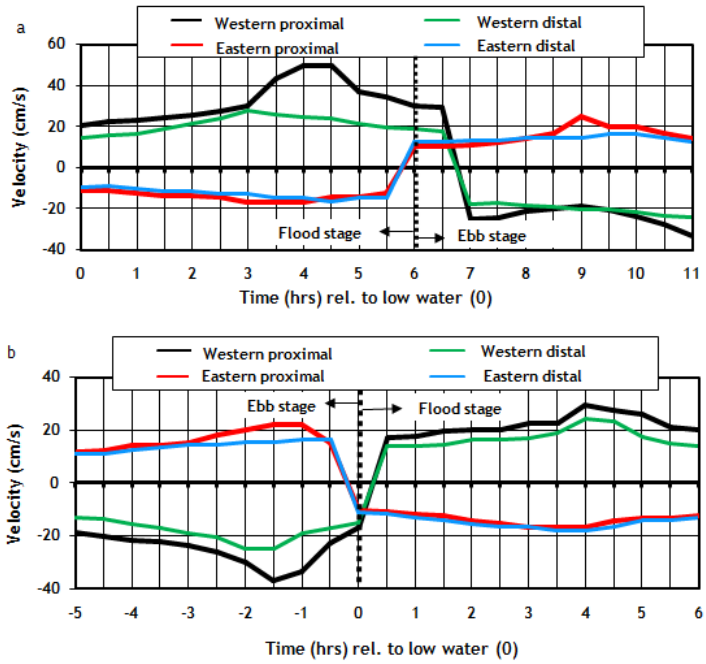

Figure 5. Tidal cycle variation in longshore residual flow velocities in western and eastern estuary-proximal and -distal surf zones of Itak Abasi and Ibeno Beach at a) neap tide (February 1) and b) spring tide (February 8, 2012). Vertical discontinuous lines mark transition between tidal stages.

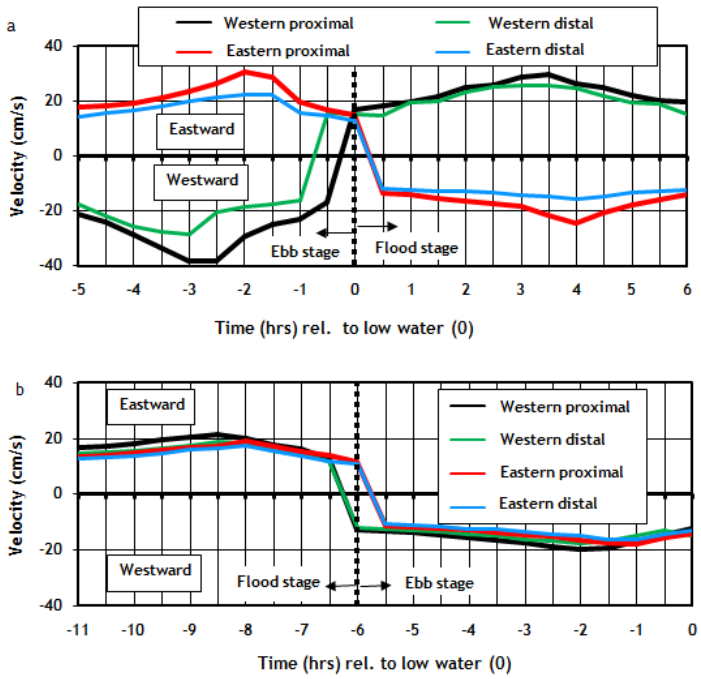

Figure 6. Tidal cycle variation in longshore residual flow velocities in western and eastern estuary- proximal and distal surf zones of Itak Abasi and Ibeno Beach at a) spring tide (March 9). and b) neap tide (March 16, 2012). Vertical discontinuous lines mark transition between tidal stages.

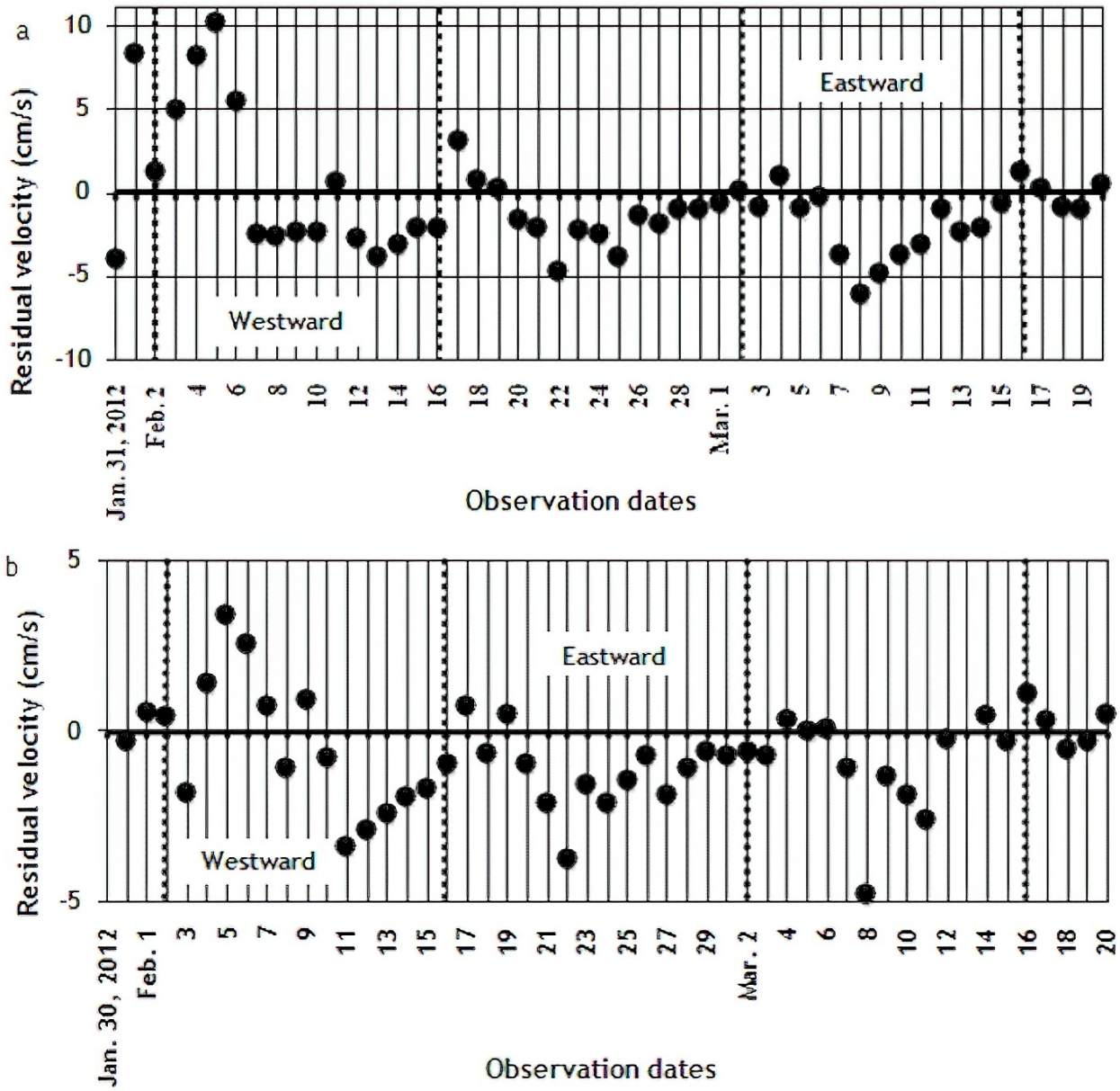

Figure 7. Variation in tidal cycle-averaged residual flow velocities of a) western Itak Abasi Beach proximal surf zone (January 30–March 20, 2012), b) western Itak Abasi Beach distal surf zone (January 30–March 20, 2012), c) eastern Ibeno Beach proximal surf zone (February 1–March 20, 2012), d) eastern Ibeno Beach distal surf zone (January 31–March 20, 2012). Vertical discontinuous lines mark neap tides.

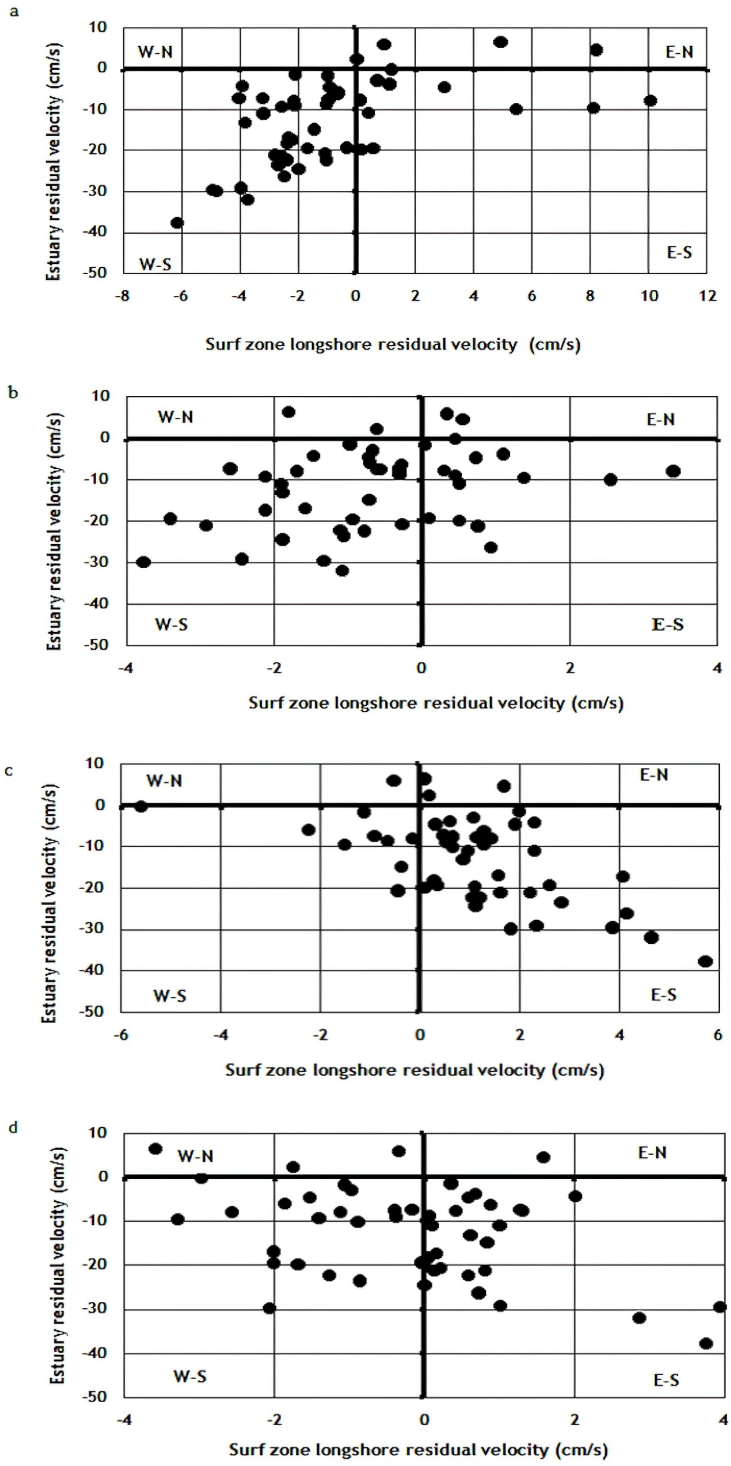

Figure 8. Scatter plot of tidal cycle residual flow vectors (January 31–March 20, 2012) for a) Qua Iboe River estuary and western Itak Abasi Beach proximal surf zone, b) Qua Iboe River estuary and western Itak Abasi Beach distal surf zone, c) Qua Iboe River estuary and eastern Ibeno Beach proximal surf zone, d) Qua Iboe River estuary and eastern Ibeno Beach distal surf zone (E – East; W – West; S – South; N – North).

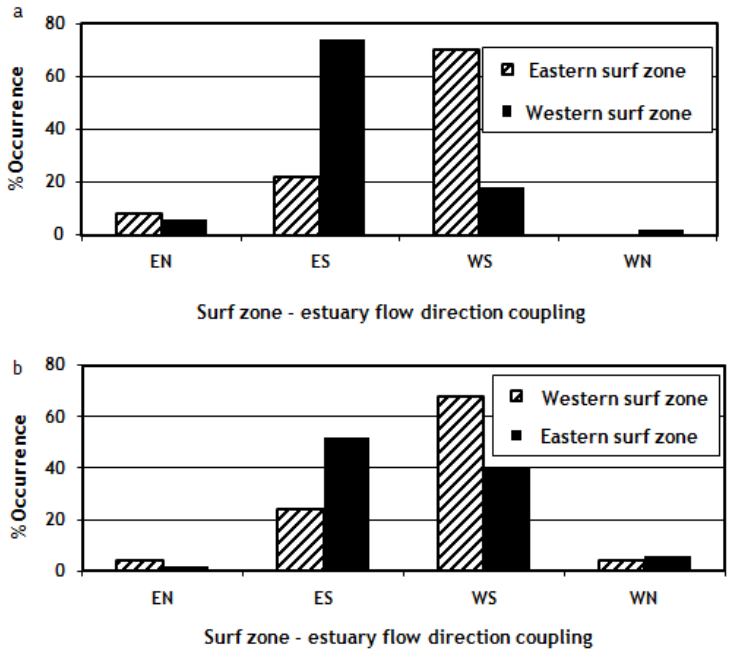

Figure 9. Histogram of frequency of directional coupling of a) estuary and western Itak Abasi Beach and eastern Ibeno Beach proximal surf zone flow, b) estuary and western Itak Abasi Beach and eastern Ibeno Beach distal surf zone flow for the study period (E – East; W – West; S – South; N – North).

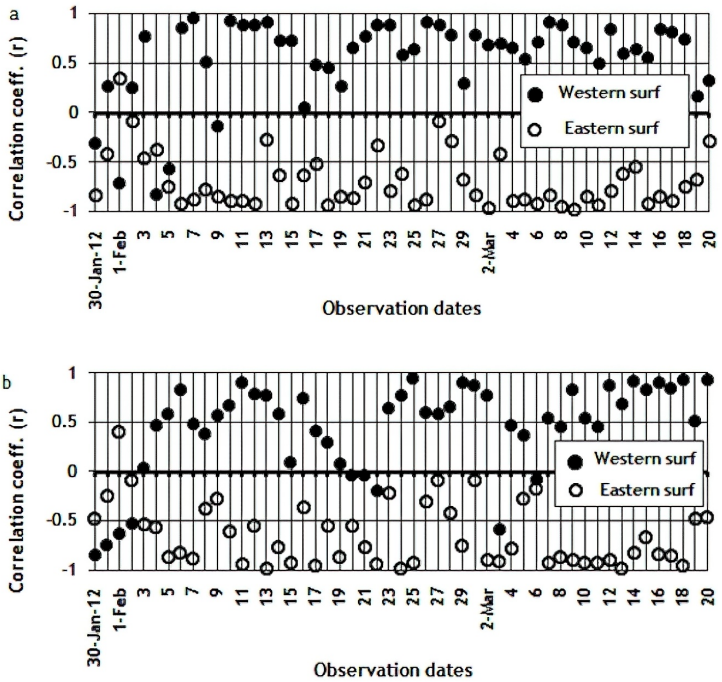

Figure 10. Correlation of ebb-tidal stage flow velocity vectors of a) Qua Iboe River estuary and proximal western (Itak Abasi) and eastern (Ibeno) surf zones, b) Qua Iboe River estuary and distal western (Itak Abasi) and eastern (Ibeno) surf zones for the study period.

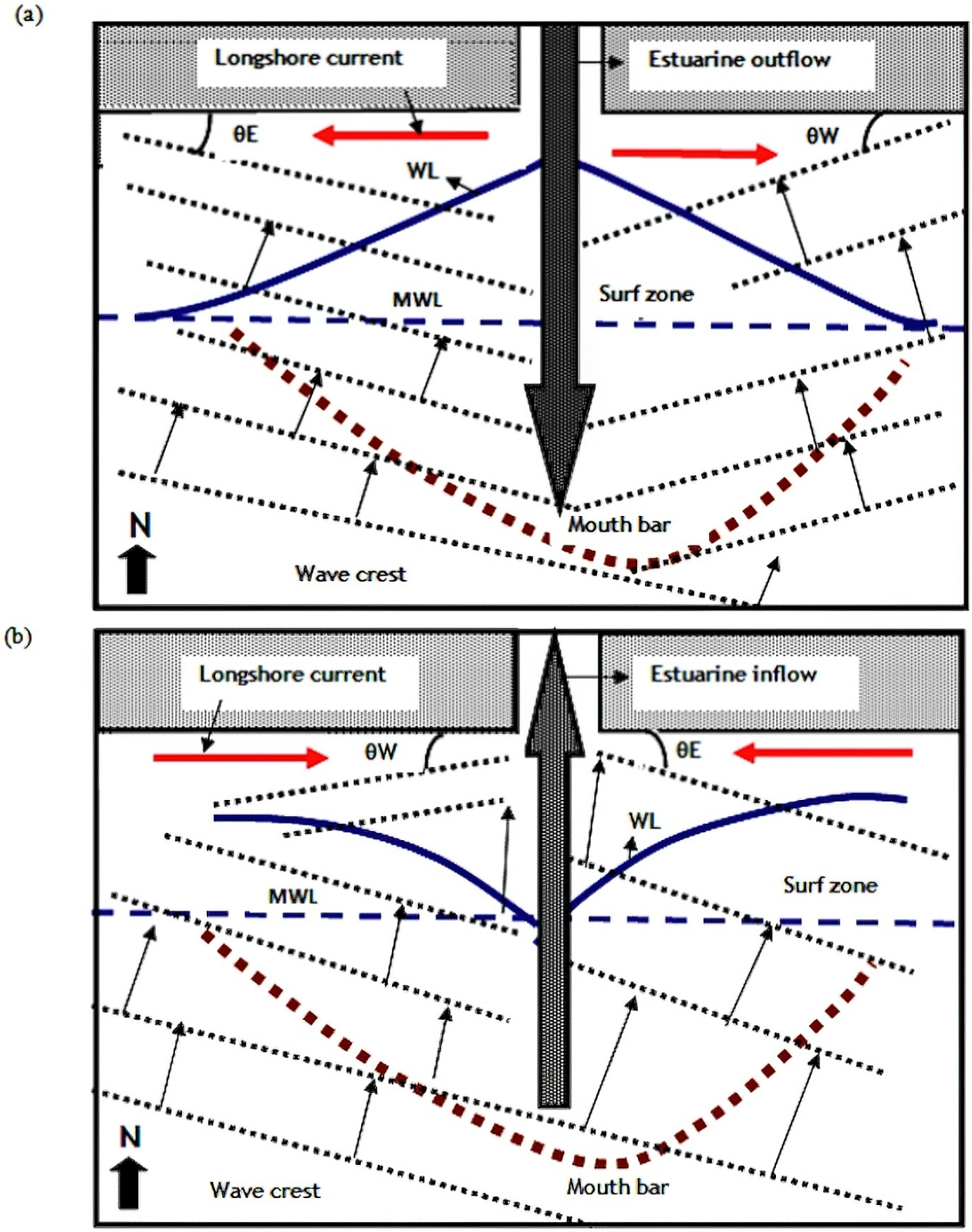

Figure 11. Pattern of western and eastern surf zone longshore flow at a) ebb stage of estuarine outflow and b) flood stage of estuarine inflow. MWL is surf zone mean water level; WL is instantaneous wave-driven water level; θE and θW are eastward- and westward-facing wave breaker angles.

The strength of coupling between the estuarine flow and the proximal surf zone flows as statistically evaluated from their measured flow vectors over 50 tidal cycles is presented for ebb and flood stages in Figure 10a–b. Also evident is that in the western surf zone, the flow vectors showed a predominantly positive correlation with the estuarine counterpart, while the eastern counterpart showed a predominantly negative correlation, implying that the direction of longshore flow in both surf zones is a mirror image of each other. The positive correlation coefficient values indicate that the estuarine outflow (negative sign) correlates with the westward (negative sign) longshore flow, while the negative correlation coefficient indicates that estuarine outflow (negative sign) correlates with the eastward (positive sign) longshore flow. During the ebb stage, the longshore and estuarine flow had a threshold correlation coefficient $r \geq 0.7$ in 50% of the data on the estuary-proximal western surf zone as against 64% for the eastern surf zone counterpart. The corresponding values at their respective distal surf zones were 48% and 66%.

During the flood stage of northward estuarine inflow (positive sign), proximal surf zone – estuarine flow coupling (Figure 10b) indicated a similar pattern to that of the ebb stage but a lower frequency of data exceeding the threshold correlation coefficient. The western surf zone with eastward longshore flow had 36% of data above threshold correlation coefficient as against 56% at the eastern surf zone where the longshore flow was westward, implying convergence of surf zone longshore flows towards the estuary mouth. The corresponding values at the distal surf zones were 38% and 50%, respectively.

4. Discussion

The results presented earlier show that flow in both the estuary and the adjoining surf zones reverses within tidal frequencies. Of particular interest is the origin of the coupling pattern between the estuarine and surf zone flows.

4.1 Tidal stage flow pattern

This ebbing stage was marked by southward (ocean-ward) residual flow from the Qua Iboe River estuary. Flow during this tidal stage at the western surf zone (Itak Abasi Beach) had 70% of the residual velocity data directed westward at the proximal surf zone and 68% at the distal counterpart. This means that over a tidal cycle, the averaged westward longshore flow was mostly swifter than the eastward counterpart. By contrast, 74% eastward residual longshore flow on the eastern proximal surf zone (Ibeno Beach) will imply that the averaged westward flow was less swift. This frequency decreased to 60% at the distal surf zone.

The fact that longshore flow in the surf zone reverses in direction within tidal frequencies under the same wave regime suggests that their mechanisms of generation vary with the tidal stage. In the case of the western surf zone, longshore flow at the ebb stage results from a westward-directed shore-parallel pressure gradient (Figure 11a) developed when the estuarine outflow is trapped in the surf zone by the water mass associated with the southwesterly shoaling waves (Antia, 2024). This is attested to by the lower intensity of westward residual longshore currents at neap tide than at spring tide (February 8, February 22 and March 9) in Figure 7a–b, largely because the southerly residual estuarine flows are also much swifter at spring than neap tide (Figure 4).

However, the expectation that during flood stage the southwesterly waves will propagate to breaker point and generate eastward longshore currents was shown to be inconsistent with the predominantly westward-facing breaker angle (Antia, 2024). A more likely mechanism compatible with the westward-facing breaker angle is eastward-directed shore-parallel pressure gradient developed when the estuarine inflow drags a segment of the wave crest within its strongest influence resulting in differential in water elevation in the surf zone (Figure 11b). The pressure gradient at flood stage will in most cases be milder than that of the ebb stage counterpart. Consequently the tidal cycle longshore flow residual on the western surf zone will be mostly westward.

On the eastern surf zone, where the ebb-stage longshore current is eastward, Antia (2024) showed that this current direction was inconsistent with the westward-facing breaker angle. Consequently, it was postulated that refraction of southwesterly waves by mouth bar morphology (and possibly the estuarine outflow) to southeasterly on the eastern shoreface enhanced the trapping of the estuarine outflow, thereby creating an eastward-directed pressure gradient driving the longshore flow as shown in Figure 11a. However, at an ebb stage, the westward longshore flow may result from at least two mechanisms. The first is the estuary mouth bar refraction of southwesterly waves to southeasterly in which case the momentum flux of the breaking waves is westward-directed. Due to the predominantly eastward-facing breaker angle at this tidal stage reported by Antia (2024), this mechanism is not primary. The second mechanism as detailed by the latter and represented in Figure 11b requires the development of westward-directed pressure gradient which is a consequence of differential drag of the segment of the shoaling southwesterly within the strongest influence of the estuarine inflow. This segment creates a lower water level than the portion of crest experiencing less drag. This mechanism is compatible with the reported eastward-facing breaker angle.

The tidal cycle residual longshore flow eastward in the eastern surf zone indicates that the pressure gradient at ebb stage is stronger than at flood stage. Finally, unlike the southward residual flow, the northward (upstream-ward) residual flow in the estuary rarely occurred (Figure 4) and thus this directional coupling with surf zone longshore

residual flows is represented in < 10% of the data set.

4.2 Strength of estuarine–surf zone hydrodynamic coupling and implications

From the results in Figure 10 and based on the correlation coefficient threshold of $r \geq 0.7$, the estuarine flow modulates more the longshore flow in the eastern surf zone than the western counterpart. This is evident from the higher frequency of the former having a contrast relative to the latter of 14% at ebb and 20% at flood tidal stages in the proximal surf zones. The distal surf zone also showed a contrast ranging from 18% at an ebb stage to 12% at a flood stage. This result will have implications for the relative dispersal and concentration of estuary-emanating pollutants across both surf zones. In particular, the retention of estuarine-emanating effluents will be higher in the eastern than western surf zone.

The surf zone – estuarine coupling of residual flow velocities in Figure 9 is more pronounced for the estuarine outflow than inflow, such that surf zone flows are typically divergent during estuarine outflow. This tidal cycle residual flow pattern will play a significant role over a long time in the development and stability of the estuarine mouth bar, which currently extends close to 1.7 km from the shoreline (Figure 1), compared to about 800 m in 2007 imagery. This river mouth bar progradation translates to an annual (2007–2013) average of 150 m.

Given that the surf zone width in the study area seldom extend beyond 100 m from the shoreline, the eastward-skew of the mouth bar configuration is unlikely to be wholly the result of the breaking wave-generated eastward currents in the western surf zone. Moreover, the tidal cycle residual flow is westward and relatively weak (< 5 cm/s). Consequently, a plausible cause for the eastward asymmetry of the estuarine mouth bar is the effect of the eastward-directed momentum flux associated with water mass transport of the obliquely-shoaling southwesterly waves on the western shoreface.

5. Conclusions

The pattern of estuarine – surf zone hydrodynamic coupling was examined in a field setting marked by reversing flow directions at tidal frequencies. Results show that the estuarine residual outflow acts as an expanding jet such that surf zone residual longshore flows have 60–70% westward-asymmetry on the western surf zone (Itak Abasi Beach) flanking the Qua Iboe River estuary as against 54–78% eastward-asymmetry on the eastern flanking surf zone of Ibeno Beach. The lower frequencies occurring at the distal surf zone monitoring stations suggests diminishing influence of the estuarine jet. The observed pattern of surf zone flow is inconsistent with the predicted eastward-directed longshore current given the predominantly southwesterly breaking waves in the surf zone. The divergent surf zone longshore flow during the estuarine outflow stage is amenable to explanation by interaction of the southwesterly waves with both the estuarine outflow as well as the estuary mouth bar morphology.

Statistical analysis shows surf zone – estuarine flow vector correlation coefficient $r \geq 0.7$ in 50% of the western surf zone data and 64% on the eastern counterpart at ebb stage, as against 36% and 56% respectively at flood stage. This indicates that estuarine outflow is a more effective modulator of surf zone flow pattern than the flood currents. The pattern of strong estuarine residual outflow velocities and modally divergent weak surf zone flow counterparts is considered a favourable condition for estuary mouth bar development and stability in the study area. Given the weak and westward residual longshore flow in the western surf zone, the eastward-asymmetric configuration of the estuary mouth bar is more likely a response to processes beyond the < 100m-wide surf zone of breaking waves. Such a process is related to the interaction between the highly dissipated momentum flux of the estuarine jet in the offshore region and the stronger eastward-directed momentum flux associated with water mass transport of the obliquely-shoaling southwesterly waves on the western shoreface.

Acknowledgements

Thanks to the Nigerian Geological Survey Agency for funding coastal investigation projects of the National Centre for Marine Geosciences under the direction of the author over the period 2007–2012 of which this study is an offshoot. Well appreciated are Henry Etukedung and Umana Umana for field logistics support as well as in field monitoring, while Effiom Oyo and Charles Effiom provided assistance in data collation.

Declaration of interest

None declared.

References

Anthony, E. J., 2015. *Wave influence in the construction, shaping and destruction of river deltas: a review*. Mar. Geol. 361, 53–78. https://doi.org/10.1016/j.margeo.2014.12.004

Antia E. E., 2024. *On reversal of wave-generated longshore currents at tidal frequencies on dissipative beaches contiguous to a mesotidal estuary, S. E coast of Nigeria*. Mar. Geol. 477(5):107389. https://doi.org/10.1016/j.margeo.2024.107389

Chao, S.–Y., 1990. *Tidal modulation of estuarine plumes*. J. Phys. Oceanogr. 20(7), 1115–1123.

Davis, R. A., Fox, W.T., 1981. Interaction between wave- and tide-generated processes at the mouth of a microtidal estuary: Matanzas River, Florida (USA). Mar. Geol. 40(1–2), 49–68. https://doi.org/10.1016/0025-3227(81)90042-6

Dodet, G., Bertin, X., Bruneau, N., Fortuato, A. B., Nahon, A., Roland, A., 2013. *Wave-current interactions in a wave-dominated tidal inlet*. J. Geophys Res.-Oceans 118, 1597–1605. https://doi.org/10.1002/jgrc.20146.2013

Finley, R. J., 1978. *Ebb-tidal delta morphology and sediment supply in relation to seasonal wave energy flux, North Inlet, South Carolina*. J. Sediment. Res. 48 (1), 227–238. https://doi.org/10.1306/212F743C-2B24-11D7-8648000102C1865D

FitzGerald, D. M., 1984. *Interactions between the ebb-tidal delta and landward shoreline: Price Inlet, South Carolina*. J. Sediment. Petrol. 54(4), 1303–1318.

Guillou N., Chapalain, G., 2012. *Effects of tide on waves in the outer seine estuary and the harbor of Le Havre*. Coast Eng. Proc. 1(33). https://doi.org/10.9753/ice.v33.waves.47

Hansen, J. E., Elias, E., List, J. H., Erikson, L. H., Barnard, P. L., 2013. *Tidally influenced alongshore circulation at an inlet-adjacent shoreline*. Cont. Shelf Res. 56, 26–38.

Hayes, M. O., 1979. *Barrier island morphology as a function of tidal and wave regime*, [in:] Leatherman, S. P. (ed.), *Barrier Islands from the Gulf of St. Lawrence to the Gulf of Mexico*. Acad. Press, New York, 1–27.

Hayes, M. O., 1980. *General morphology and sediment patterns in tidal inlets*. Sediment. Geol. 26, 139–156.

Hughes, S. A., 2002. *Estimating surface currents near coastal structure using dye and drogues*. EDC/CL CHETN-V1-37, U.S. Army Eng. Res. Dev. Ctr, Vicksburg, MS. 14 pp. http://chl.wes.army.mil/library/publications/chetn

Joshi, P. B., 1982. *Hydromechanics of tidal jets*. J. Waterw, Port C-ASCE 108(3), 239–253.

Oertel, G. F.,1975. *Ebb tidal deltas of Georgia estuaries*, [in:] Cronin, L. E. (ed.), *Estuarine Research*, Acad. Press, New York, San Francisco, London, 267–276.

Olabarrieta, M., Geyer, R., Kumar. N., 2014. *The role of morphology and wave-current interaction at tidal inlets: an idealized modeling analysis*. J. Geophys. Res.-Oceans 119(12), 8818–8837.

Ozsoy, E., Unluata, U., 1982. *Ebb-tidal flow characteristics near inlets*. Estuar. Coast Shelf Sci. 14(3), 251–263.

Rusu, L., Bernardino, M., Guedes, S. C., 2011. *Modelling the influence of currents on wave propagation at the entrance of Tagus estuary*. Ocean Eng. 38, 1174–1183.

Sha, L. P., van der Berg, J. H., 1993. *Variation in ebb-tidal delta geometry along the coast of the Netherlands and the German Bight*. J. Coast. Res. 9, 730–746.

Todd, T. W., 1968. *Dynamic diversion: influence of longshore current-tidal flow interaction on chernier and barrier island plains*. J. Sediment. Petrol. 38, 734–746.

Zainescu, F., Anthony, E. J., Vespremeanu-Stroe, A., 2021. *River jets versus wave-driven longshore currents at river mouths*. Front. Mar. Sci. 8, 708258. https://doi.org/10.3389/fmars.2021.708258